

The Stellar Halo Metallicity – Luminosity Relationship for Spiral Galaxies

Agostino Renda^{1*}, Brad K. Gibson^{1,6*}, Mustapha Mouhcine², Rodrigo A. Ibata³, Daisuke Kawata^{1,7†}, Chris Flynn^{1,4}, Chris B. Brook^{1,5}

¹Centre for Astrophysics & Supercomputing, Swinburne University, Hawthorn, Victoria 3122, Australia

²School of Physics and Astronomy, University of Nottingham, University Park, Nottingham NG7 2RD, UK

³Observatoire Astronomique de Strasbourg, 11, rue de l’Université, 67000 Strasbourg, France

⁴Tuorlan Observatorio, Väisäläntie 20, 21500 Piikkiö, Finland

⁵Département de Physique, de Génie Physique et d’Optique, Université Laval, Québec G1K 7P4, Canada

⁶School of Mathematical Sciences, Monash University, Clayton, Victoria 3800, Australia

⁷The Observatories of the Carnegie Institution of Washington, 813 Santa Barbara Street, Pasadena, CA 91101, USA

Accepted. Received; in original form

ABSTRACT

The stellar halos of spiral galaxies bear important chemo–dynamical signatures of galaxy formation. We present here the analysis of 89 semi–cosmological spiral galaxy simulations, spanning ~ 4 magnitudes in total galactic luminosity. These simulations sample a wide variety of merging histories and show significant dispersion in halo metallicity at a given total luminosity – more than a factor of ten in metallicity. Our preliminary analysis suggests that galaxies with a more extended merging history possess halos which have younger and more metal rich stellar populations than the stellar halos associated with galaxies with a more abbreviated assembly. A correlation between halo metallicity and its surface brightness has also been found, reflecting the correlation between halo metallicity and its stellar mass. Our simulations are compared with recent Hubble Space Telescope observations of resolved stellar halos in nearby spirals.

Key words: galaxies: halos – galaxies: formation – galaxies: evolution – galaxies: structure – numerical methods

1 INTRODUCTION

Understanding the formation history of stellar halos is one of the classical pursuits of galactic astronomy. The problem is generally framed within the context of two competing scenarios: one of “rapid collapse” (Eggen, Lynden–Bell & Sandage 1962), in which the stellar halo is formed by the rapid collapse of a proto–galaxy within a dynamical timescale ($\sim 10^8$ yr), and one of “galactic assembly” (Searle & Zinn 1978), whereby the stellar halo is assembled on a longer timescale ($\sim 10^9$ yr) by the accretion of “building–blocks”, each with separate enrichment histories. Both scenarios have their strengths and weaknesses, and it would appear that a hybrid model is the most plausible option consistent with extant data (e.g.: Chiba & Beers 2000; Freeman & Bland–Hawthorn 2002).

An intriguing piece of the halo formation “puzzle” is provided by comparing the stellar halo of our own Milky

Way with that of its neighbour, M31. First, despite their comparable total galactic luminosities, the stellar halo of M31 is *apparently* much more metal–rich than that of the Milky Way (e.g.: Ryan & Norris 1991; Mould & Kristian 1986; Durrell, Harris & Pritchett 2001; Ferguson et al. 2002; Brown et al. 2003; Bellazzini et al. 2003; Durrell et al. 2004; Ferguson et al. 2005; Irwin et al. 2005). In fact, the halo of M31 bears a closer resemblance to that of NGC 5128 (e.g., Harris & Harris 2001), despite their differing morphological classifications.

The stellar halo – galaxy formation symbiosis has been further brought to light by the recent work of Mouhcine et al. (see also Tikhonov, Galazutdinova & Drozdovsky 2005). The deep Hubble Space Telescope (HST hereafter) imaging of nearby spiral galaxy stellar halos in Mouhcine et al. (2005) suggests a significant correlation between stellar halo metallicity and total galactic luminosity. On the surface, this correlation appears to leave our own Milky Way’s halo as an outlier with respect to other spirals, with a stellar halo metallicity ~ 1 dex lower than spirals of comparable luminosity (such as M31, as alluded to earlier).

* E–mail: arenda,bgibson@astro.swin.edu.au

† E–mail: dkawata@ociw.edu

However, it must be noted that the metallicity of the Galactic halo in the Solar Neighbourhood (e.g., in Ryan & Norris 1991) comes from spectroscopic metallicities in a kinematically-selected sample, whereas that of the M31 halo, as well as those of the stellar halos of nearby spiral galaxies (Mouhcine et al. 2005), have been derived primarily from photometric metallicities in geographically-selected samples. Because it is now becoming possible to obtain spectroscopic metallicities for significant samples of kinematically-selected giants in the M31 halo (e.g.: Ibata et al. 2004; Guhathakurta et al. 2005), it will be crucial to assess the consistency of the M31 stellar halo metallicity as derived from kinematically- and from geographically-selected samples, respectively.

A grasp of the true scatter around the general trend in the halo metallicity – luminosity relation awaits a larger observational data set, however any theory which attempts to explain such a relation needs to simultaneously account for the *apparent* metallicity discrepancy between the Milky Way and the Andromeda stellar halos. The question arises as to what is driving the scatter of halo metallicity for galaxies of comparable luminosity?

In what follows, we investigate whether differences in the stellar halo assembly history can explain the diversity seen in halo metallicities. Using chemo-dynamical numerical simulations, we have constructed a sample of 89 model disc galaxies, spanning ~ 4 magnitudes in luminosity, and sampling a wide range of assembly histories at a given luminosity (or mass). We contrast the derived stellar halo metallicity – galactic luminosity relation with the recent empirical determination of Mouhcine et al. (2005). The numerical framework in which the simulations have been conducted is described in Section 2, while Sections 3 and 4 present the results and the related discussion, respectively.

2 SIMULATIONS

The simulations employed here are patterned after the semi-cosmological adiabatic feedback model of Brook et al. (2004), and were constructed using the chemo-dynamical code **GCD+** (Kawata & Gibson 2003). **GCD+** self-consistently treats the effects of gravity, gas dynamics, radiative cooling, star formation, and chemical enrichment (including Type II and Ia Supernovae, relaxing the instantaneous recycling approximation).

This semi-cosmological version of **GCD+** is based on the seminal work of Katz & Gunn (1991). The initial condition for a given model is an isolated sphere of dark matter and gas. This “top-hat” overdensity has an amplitude δ_i at initial redshift z_i , which is approximately related to the collapse redshift z_c by $z_c = 0.36\delta_i(1 + z_i) - 1$ (e.g., Padmanabhan 1993). We set $z_c = 2.0$, which determines δ_i at $z_i = 40$. Small-scale density fluctuations based on a CDM power spectrum are superimposed on the sphere using **COSMICS**¹ (Bertschinger 1998), and the amplitude of the fluctuations is parameterised by σ_8 . These fluctuations are the seeds for local collapse and subsequent star formation. Solid-body rotation corresponding to a spin parameter λ is

imparted to the initial sphere to incorporate the effects of longer wavelength fluctuations. For the flat CDM model described here, the relevant parameters include $\Omega_0 = 1$, baryon fraction $\Omega_b = 0.1$, $H_0 = 50 \text{ km s}^{-1} \text{ Mpc}^{-1}$, spin parameter $\lambda = 0.06$, and $\sigma_8 = 0.5$. We employed 14147 dark matter and 14147 gas/star particles, for the 89 simulations presented here.

Using the same number of particles, collapse redshift z_c , and spin parameter λ , a series of 89 simulations were completed spanning a factor of 50 in mass in four separate mass “bins”: $M_{\text{tot}} = 1 \times 10^{11} M_\odot$; $5 \times 10^{11} M_\odot$; $1 \times 10^{12} M_\odot$; $5 \times 10^{12} M_\odot$. For each total mass, we run models with different patterns of small-scale density fluctuations which lead to different hierarchical assembly histories. This was controlled by setting different random seeds for the Gaussian perturbation generator in **COSMICS**.

3 RESULTS

Our grid of 89 simulations were employed to populate the redshift $z = 0$ stellar halo metallicity – luminosity plane (i.e. $\langle [\text{Fe}/\text{H}] \rangle_{\text{halo}} - M_V$) shown in Fig. 1 (filled symbols²). We have been conservative in our geometrical definition of “stellar halo”, adopting a projected cut-off radius of 15 kpc to delineate the halo from (possible) disc-bulge contaminants. Such a choice should also allow an easier comparison with the observations of halo fields in nearby spiral galaxies.

The stellar metallicity distribution function (MDF) was then generated using all stellar particles from the halo “region”, convolved with a Gaussian of $\sigma_{[\text{Fe}/\text{H}]} = 0.15$ dex, representing the typical observational uncertainties (e.g., Bellazzini et al. 2003). The peaks of the derived MDFs are shown³ in Fig. 1; 68% of the stellar particles within a given (simulated) MDF typically span 1.4 dex in metallicity. We confirmed that the derived halo MDFs are insensitive to projection effects, even in the most massive (largest) models, suggesting that our $R \sim 15$ kpc definition for the halo “region” is sufficient for minimising disc and bulge contamination. The optical properties of our simulated stellar populations were derived using the population synthesis models of Mouhcine & Lançon (2003), taking into account the age and the metallicity of each stellar particle. We note that the V-band luminosity shown along the abscissa of Fig. 1 is the *total* galactic luminosity (i.e. halo + bulge + disc).

Fig. 1 also shows the corresponding observed halo metallicity – luminosity values for 13 nearby spirals, taken primarily from Mouhcine et al. (2005), supplemented with data from the literature (Binney & Merrifield 1998; Elson 1997; Harris, Harris & Poole 1999; Brooks, Wilson & Harris 2004)⁴. For the observational datasets, we calculated the MDF peak and 68% “dispersions” exactly as we did for the

² Note: MDF centroids were constrained to sit on a 0.2 dex “grid” in $\langle [\text{Fe}/\text{H}] \rangle_{\text{halo}}$, which is the source of the apparently “quantised” centroid values in Fig. 1.

³ Only those simulations with > 100 halo stellar particles are included in the analysis here.

⁴ Note that the identification of the stellar halo in M33 is still debated (e.g., Tiede, Sarajedini & Barker 2004).

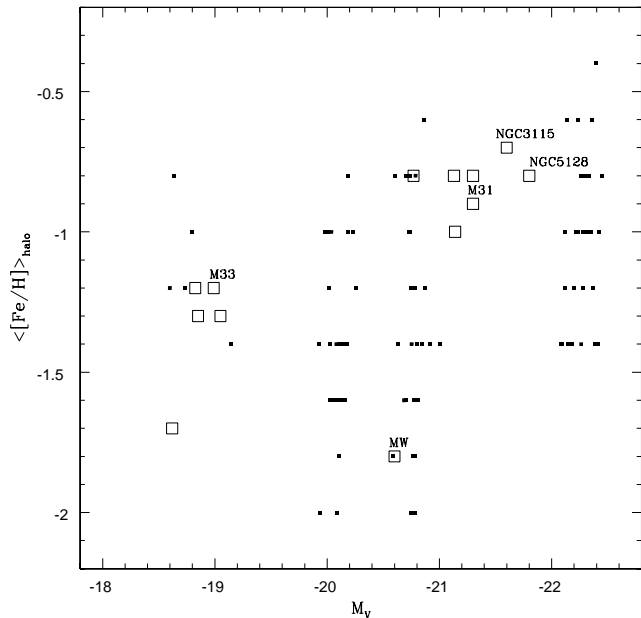


Figure 1. The stellar halo metallicity – total galactic V-band luminosity relation ($\langle [\text{Fe}/\text{H}] \rangle_{\text{halo}} - M_V$). Filled squares correspond to the peak of the MDF for each of our simulations. Open (unlabelled) squares represent the data of Mouhcine et al. (2005); open (labelled) squares represent additional data taken from the literature (see the text for details). 68% of the stars in the simulated (observed) MDFs are typically enclosed within ± 0.7 dex (± 0.35 dex) of the peak of the respective MDF.

simulated datasets⁵; 68% of the stars in the observed MDFs are typically enclosed within ± 0.35 dex of the MDF peak, a factor of ~ 2 narrower than the simulations⁶.

What is readily apparent from Fig. 1 is that significant variation in halo metallicity ($\gtrsim 1$ dex) exists at any given total galactic luminosity in our simulations. For a set of models with the same initial total mass, the only difference among these models can be traced to the random pattern of initial small-scale density fluctuations; this translates directly into differing hierarchical assembly histories. Qualitatively, it would appear that assembly history alone may account for the diversity in halo metallicity at a given galactic luminosity, and thus account for the apparent outliers in the observed trend.

Fig. 2 shows snapshots of the gas particles at redshift z

⁵ Each MDF has been fitted by an univariate skew-normal distribution (e.g.: Azzalini 2005; <http://azzalini.stat.unipd.it/SN/Intro/intro.html>). For the observational datasets, we calculated the MDF as derived from the mean location of the Red Giant Branch stars in the Colour Magnitude Diagrams of the fields observed in Mouhcine et al. (2005).

⁶ Our current model does not take into account any pre-enrichment scenario due to extremely metal-poor stars (Pop III hereafter) whose detailed physics is still much debated (e.g.: Woosley, Heger & Weaver 2002; Larson 2005). An early and homogeneous pre-enrichment of the proto-galactic masses due to Pop III could lead to narrower MDFs at lower redshift.

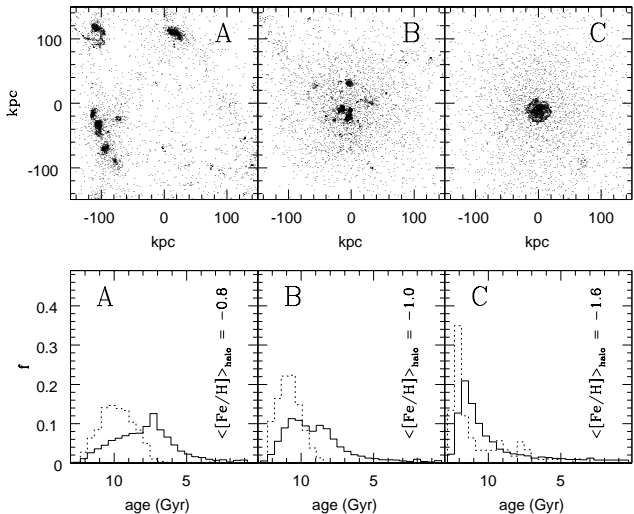


Figure 2. *Upper panels:* Projected distribution of the gas particles at redshift $z = 1.5$ for the simulations with $M_{\text{tot}} = 10^{12} M_{\odot}$. *Lower panels:* The associated stellar age distributions at $z = 0$ for the galaxies in the upper panels. The solid (dotted) histogram corresponds to the stellar age distribution for the entire galaxy (stellar halo). The corresponding halo metallicities are denoted in each panel.

$= 1.5$ and the associated $z = 0$ stellar Age Distribution Function (ADF) for three of the models with $M_{\text{tot}} = 10^{12} M_{\odot}$. These representative models demonstrate that the simulated galaxies with the more metal-rich halos are assembled over a longer timescale, and thus possess a broader ADF (both in the halo and in the associated galaxy). Such a scenario is consistent with the evidence, presented by Brown et al. (2003), of a substantial intermediate-age metal-rich population in a geographically-selected halo field of M31⁷. Conversely, the simulated galaxies with the more metal-poor halos are assembled earlier through more of a monolithic process, with a consequently narrower ADF. Our simulations suggest that the halo metallicity reflects directly the formation and assembly history of the host galaxy⁸.

Further, the most metal-poor stellar halos in our simulations (which, recall, formed preferentially via more of a monolithic collapse) possess α -elements to iron ratios a factor of ~ 2 higher than the most metal-rich halos (which formed preferentially over more extended period of hierar-

⁷ However, the eventual contamination (by the disc or by debris of accreted satellites) in this outer field is debated (e.g.: Brown 2003; Ferguson et al. 2005).

⁸ We note that the “dispersion” in the halo and total galactic ADFs appear correlated, such that galaxies with narrower halo ADFs also appear to have narrower total galactic ADFs. This could suggest that the assembly history of the halo “knows” of the formation history of the other galactic structural components (e.g., bulge and disc). We will explore this suggestion in a future study.

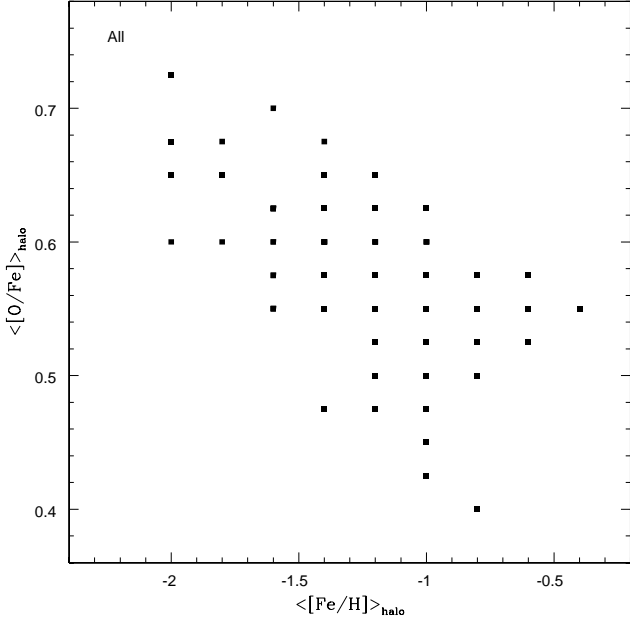


Figure 3. The relation between the peak of the halo $[O/Fe]$ distribution function and the peak of the halo MDF in our simulations.

chical clustering), as shown in Fig. 3. Such a trend is expected if the different amount of α -elements and Iron released by Type II and Ia Supernovae over different timescales is taken into account (e.g.: Timmes, Woosley & Weaver 1995; Woosley et al. 2002).

The upper panels of Fig. 4 show the stellar halo metallicity – I-band surface brightness relation ($\langle [Fe/H] \rangle_{\text{halo}} - \mu_{\text{I}}^{\text{halo}}$) for models with $M_{\text{tot}} = 10^{12} M_{\odot}$; the surface brightness was measured at a projected distance of 20 kpc from the dynamical centre of each simulation. The halo metallicity – stellar mass relation ($\langle [Fe/H] \rangle_{\text{halo}} - M_{*}^{\text{halo}}$) is shown in the lower panels of Fig. 4. The three galaxies presented in Fig. 2 are also labelled in Fig. 4. An immediate correlation is apparent with the more massive halos possessing higher surface brightness and also higher metallicity. This is consistent with a picture in which galaxies that experienced more extended assembly histories have more massive stellar halos, with both higher halo metallicities and halo surface brightnesses - i.e. higher stellar halo densities. Similar trends are observed in our other total mass models, as shown in the right panels of Fig. 4.

The issue of model convergence (resolution) is always a concern when interpreting cosmological simulations (particularly when including baryons). To test this, we conducted a series of simulations for $M_{\text{tot}} = 10^{12} M_{\odot}$, with 5575×2 and 9171×2 particles, to supplement the default grid (which used 14147×2 particles); the middle panels of Fig. 4 show where these lower-resolution simulations sit in the halo metallicity – surface brightness plane and in the halo metallicity – stellar mass plane, respectively. The consistency between higher (left panels) and lower (middle panels) resolution models is

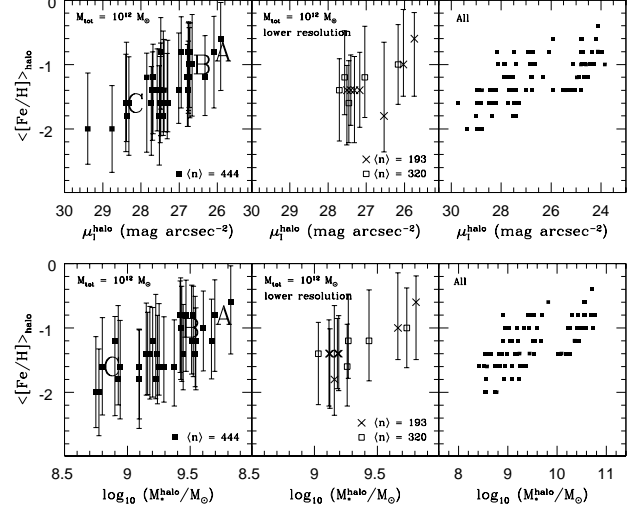


Figure 4. *Upper panels:* Stellar halo metallicity – halo I-band surface brightness relation ($\langle [Fe/H] \rangle_{\text{halo}} - \mu_{\text{I}}^{\text{halo}}$): in the left panel, our fiducial models with $M_{\text{tot}} = 10^{12} M_{\odot}$ and 14147×2 particles are shown, while the middle panel shows the corresponding lower-resolution models with 5575×2 (crosses) and 9171×2 (open squares) particles. The metallicity error bars indicate the 68% Confidence Level. The average number of halo particles is shown in the bottom right corner of each panel. Models with fewer than 100 stellar halo particles ($R > 15$ kpc) are not included here. Models A – C of Fig. 2 are denoted in the left and middle panels. The right panel shows the $\langle [Fe/H] \rangle_{\text{halo}} - \mu_{\text{I}}^{\text{halo}}$ relation for all the simulations. *Lower panels:* Halo metallicity – stellar mass relation ($\langle [Fe/H] \rangle_{\text{halo}} - M_{*}^{\text{halo}}$): in the left panel, our fiducial models with $M_{\text{tot}} = 10^{12} M_{\odot}$, while the middle panel shows the corresponding lower-resolution models. The right panel shows the $\langle [Fe/H] \rangle_{\text{halo}} - M_{*}^{\text{halo}}$ relation for all the simulations.

reassuring and leads us to conclude that our simulations are not affected significantly by numerical resolution.⁹

4 SUMMARY AND CONCLUSIONS

We have presented here an analysis of the characteristics of spiral galaxy stellar halos formed within a large grid of numerical simulations, with particular emphasis placed upon the relationship between stellar halo metallicity and the associated galactic luminosity. We have demonstrated that at any given total luminosity (or, conversely, total dynamical mass), the metallicities of these simulated stellar halos span a range in excess of ~ 1 dex. We suggest that the underlying driver of this metallicity spread can be traced to the diversity of galactic mass assembly histories inherent within

⁹ Because we limit our analyses to models with >100 halo stellar particles, the $\mu_{\text{I}}^{\text{halo}} > 28$ mag arcsec⁻² region of the halo metallicity – surface brightness plane and the $M_{*}^{\text{halo}} < 10^9 M_{\odot}$ region of the halo metallicity – stellar mass plane are underpopulated by the lower-resolution models (middle panels of Fig. 4).

the hierarchical clustering paradigm. Galaxies with a more protracted assembly history possess more metal-rich and younger stellar halos, with an associated greater dispersion in age, than galaxies which experience more of a monolithic collapse.

For a given total luminosity (or dynamical mass), those galaxies with more extended assembly histories also possess more massive stellar halos, which in turn leads to a direct correlation between a stellar halo's metallicity and its surface brightness (as anticipated by earlier semi-analytical models - e.g., Renda et al. 2005). By extension, such a correlation may prove to be a useful diagnostic tool for disentangling the formation history of disc galaxies.

Recently, Mouhcine et al. (2005) have presented an observed correlation between stellar halo metallicity and total galactic luminosity, as shown in Fig. 1. The observed dispersion in the mean halo metallicity at a given galactic luminosity is *smaller* than what we find in our simulations. *However* the latter can account for the outliers in the observed trend. Since our motivation has been to study which is the effect of the pattern of the initial density fluctuations *alone* on the stellar halo features at redshift zero in simulated spiral galaxies, it is worth to note that galaxy formation, as it is observed, is an ongoing process which is the result of the interplay among different parameters, of which the pattern of initial density fluctuations (thus the merging history) is one. We have shown that the merging history *alone* may be held responsible of the dispersion in halo metallicity at a comparable total galactic luminosity, as *apparently* observed for example in our Milky Way and in Andromeda (see Section 1).

This begs the question...*Which is normal?* Our study suggests that if the stellar halo was assembled (primarily) through more of a monolithic collapse, such a low metallicity is indeed what should be expected; conversely, the fact that the M31 stellar halo is significantly metal-rich is suggestive of a more protracted assembly history. An observational consequence of these differing formation histories is the prediction that the M31 stellar halo should possess a high surface brightness; observations tentatively support this prediction (Reitzel, Guhathakurta & Gould 1998; Guhathakurta et al. 2005; Irwin et al. 2005).

Further observations are needed to tighten our grasp of the strength and scatter of the stellar halo metallicity – luminosity relation, which we have shown to be a useful diagnostic tool for disentangling the formation history of disc galaxies.

5 ACKNOWLEDGEMENTS

We thank the anonymous reviewer for careful comments which improved the manuscript. We acknowledge the financial support of the Australian Research Council through its Discovery Project and Linkage International schemes, and the Australian and Victorian Partnerships for Advanced Computing. AR acknowledges the hospitality of the Observatoire Astronomique de Strasbourg and of the Tuorlan Observatorio, and the Swinburne Supercomputer Facility support team. DK acknowledges the financial support of the Japan Society for the Promotion of Science, through a Postdoctoral Fellowship for research abroad.

REFERENCES

- Azzalini A., 2005, *Scand. J. Stat.*, 32, 159
 Bellazzini M., Cacciari C., Federici L., Fusi Pecci F., Rich M., 2003, *A&A*, 405, 867
 Bertschinger E., 1998, *ARA&A*, 36, 599
 Binney J., Merrifield M., 1998, *Galactic Astronomy*, Princeton University Press, Princeton, New Jersey, USA
 Brook C.B., Kawata D., Gibson B.K., Flynn C., 2004, *MNRAS*, 349, 52
 Brooks R.S., Wilson C.D., Harris W.E., 2004, *AJ*, 128, 237
 Brown T.M., Ferguson H.C., Smith E., Kimble R.A., Sweigart A.V. et al., 2003, *ApJ*, 592, L17
 Brown T.M., 2003, ([astro-ph/0308298](#))
 Chiba M., Beers T.C., 2000, *AJ*, 119, 2843
 Durrell P.R., Harris W.E., Pritchett C.J., 2001, *AJ*, 121, 2557
 Durrell P.R., Harris W.E., Pritchett C.J., 2004, *AJ*, 128, 260
 Eggen O.J., Lynden-Bell D., Sandage A.R., 1962, *ApJ*, 136, 748
 Elson R.A.W., 1997, *MNRAS*, 286, 771
 Ferguson A.M.N., Irwin M.J., Ibata R.A., Lewis G.F., Tanvir N.R., 2002, *AJ*, 124, 1452
 Ferguson A.M.N. et al., 2005, *ApJ*, 622, L109
 Freeman K., Bland-Hawthorn J., 2002, *ARA&A*, 40, 487
 Guhathakurta P. et al., 2005, ([astro-ph/0502366](#))
 Ibata R.A., Irwin M.J., Lewis G.F., Ferguson A.M.N., Tanvir N.R., 2001, *Nature*, 412, 49
 Ibata R.A., Chapman S., Ferguson A.M.N., Irwin M.J., Lewis G.F., McConnachie A.W., 2004, *MNRAS*, 351, 117
 Irwin M.J., Ferguson A.M.N., Ibata R.A., Lewis G.F., Tanvir N., 2005, *ApJ Letters*, in press ([astro-ph/0505077](#))
 Harris W.E., Harris G.L.H., 2001, *AJ*, 122, 3065
 Harris G.L.H., Harris W.E., Poole G.B., 1999, *AJ*, 117, 855
 Katz N., Gunn J.E., 1991, *ApJ*, 377, 365
 Kawata D., Gibson B.K., 2003, *MNRAS*, 340, 908
 Larson R.B., 2005, ([astro-ph/0406624](#))
 Mouhcine M., Lançon A., 2003, *A&A*, 402, 425
 Mouhcine M., Ferguson H.C., Rich R.M., Brown T.M., Smith T.E., 2005, submitted
 Mould J., Kristian J., 1986, *ApJ*, 305, 591
 Padmanabhan T., 1993, *Structure formation in the universe*, Cambridge University Press, Cambridge, UK
 Reitzel D.B., Guhathakurta P., Gould A., 1998, *AJ*, 116, 707
 Renda A., Kawata D., Fenner Y., Gibson B.K., 2005, *MNRAS*, 356, 1071
 Ryan S.G. Norris J.E., 1991, *AJ*, 101, 1865
 Searle L., Zinn R., 1978, *ApJ*, 225, 357
 Tiede G.P., Sarajedini A., Barker M.K., 2004, *AJ*, 128, 224
 Tikhonov N.A., Galazutdinova O.A., Drozdovsky I.O., 2005, *A&A*, 431, 127
 Timmes F.X., Woosley S.E., Weaver T.A., 1995, *ApJS*, 98, 617
 Woosley S.E., Heger A., Weaver T.A., 2002, *Reviews of Modern Physics*, 74, 1015

This paper has been typeset from a \TeX / \LaTeX file prepared by the author.